Radiation Protection Dosimetry (2015), Vol. 164, No. 1–2, pp. 57–64
Advance Access publication 19 December 2014
doi:10.1093/rpd/ncu342

30-Y FOLLOW-UP OF A Pu/Am INHALATION CASE

Christian Wernli[1,*], Jost Eikenberg[1], Olaf Marzocchi[2], Bastian Breustedt[2], Ursula Oestreicher[3], Horst Romm[3], Demetrio Gregoratto[4] and James Marsh[4]
[1]Paul Scherrer Institute (PSI), Villigen, Switzerland
[2]Karlsruhe Institute for Technology (KIT), Karlsruhe, Germany
[3]Federal Office for Radiation Protection (BfS), Oberschleissheim, Germany
[4]Public Health England (PHE), Harwell Science and Innovation Campus, UK

*Corresponding author: christian.wernli@alumni.ethz.ch

In 1983, a young man inhaled accidentally a large amount of plutonium and americium. This case was carefully followed until 2013. Since no decorporation measures had been taken, the undisturbed metabolism of Pu and Am can be derived from the data. First objective was to determine the amount of inhaled radionuclides and to estimate committed effective dose. *In vivo* and excretion measurements started immediately after the inhalation, and for quality assurance, all types of measurements were performed by different labs in Europe and the USA. After dose assessment by various international groups were completed, the measurements were continued to produce scientific data for model validation. The data have been analysed here to estimate lung absorption parameter values for the inhaled plutonium and americium oxide using the proposed new ICRP Human Respiratory Tract Model. As supplement to the biokinetic modelling, biological data from three different cytogenetic markers have been added. The estimated committed effective dose is in the order of 1 Sv. The subject is 30 y after the inhalation, of good health, according to a recent medical check-up.

HISTORY OF THE INHALATION CASE

A first paper describing the details of the accident, the early measurements and dose estimates of the Pu/Am inhalation case of 1983 at the former Federal Institute for Reactor Research in Switzerland has been published in 2007[(1)]. Immediately after accidental inhalation by a 26-y-old male technician, dose estimates were of primary interest. The results of measurements performed in various labs were used by several organisations for testing their internal dosimetry programmes for actinides. Later on, this case became mainly of scientific interest since no chelating agent was used and, even after 30 y, *in vivo* and excretion measurements were still possible. Fortunately, the person concerned accepted all these measurement procedures. Over the last few years, organ measurements were performed with highly specialised instruments at Karlsruhe Institute for Technology (KIT)[(2)] and the excretion measurements were done again at Paul Scherrer Institute (PSI)[(1)]. In addition to all the physical measurements, current cytogenetic analyses were performed at Federal Office for Radiation Protection[(3)] to complete scientific data by biological studies.

RECENT *IN VIVO* MEASUREMENTS

Instruments and method

Recent *in vivo* measurements have been performed at KIT Karlsruhe using a system of four HPGe detectors[(2)]. Two detector configurations were used: a mixed one to monitor four organs (left lung, right lung, liver and knee), and a configuration specific for the skeleton (two detectors around the skull and two detectors for the knees). The measurement time was 4000 s per configuration. The net area of the peaks was estimated according to ISO 28 218. The calculation of the activity for ^{241}Am in each organ was performed using both ICRP Man and ICRP Female as calibration phantoms, and the calibration data were obtained using MCNPX[(4)] after a validation of the method[(2)]. The analysis of the data was performed first for the mixed configuration; the results were used to correct the calculations for the skeleton configuration.

The calculation of the activities in the mixed configuration was not performed using each detector independently, because it is known that a measurable part of the counts is generated by the crosstalk between neighbouring organs and detectors. Instead, the direct and the indirect contributions and the four peak areas were used to write a system of linear equations. The solution of the system consisted of the activity in each organ.

DISCUSSION

The solution of the system of equations applied to the mixed measurement configuration produced a negative value of ^{241}Am activity in the liver, independently from the calibration phantom used, suggesting the lack of ^{241}Am in the organ. The system was therefore rewritten to exclude the liver and the solution calculated again. The final data are shown in Table 1.

The activity in the lungs calculated using the mixed configuration was used to correct the peaks recorded in the detectors around the skull. This was performed

by simulating with MCNPX the counting efficiency for photons originated in the lungs and reaching the detectors around the skull. The number of counts originated by the skeleton was therefore lowered: the net value was 3–5 % lower when using ICRP Male as calibration phantom and 8–10 % lower for ICRP Female. The different results can be explained by the higher amount of muscles in ICRP Male that acts as shield and lowers the cross-counting efficiency for the detectors around the skull. The corrected activities are listed in Table 2.

By comparing the results for the mixed detector configuration with the results for the skeleton configuration, it appears that the activity value for the skeleton is coherent only when using ICRP Female: the calibration with ICRP Man produces a discrepancy of ~30 %.

A partial explanation for the issue is related to the MCNPX simulations and the quality of the models used to reproduce the detectors: currently, they are optimised only for the front face, not for the photons impinging on the sides of the crystal. More accurate models will be available in the future.

The placement of the detectors relative to the subject affects the results heavily, and it is the most probable cause of the discrepancy between skull and knees measurements. Additional simulations found the efficiency for the skull to decrease by ~50 % for a 2-cm slide of the subject down the reclined stretcher [see the pictures in (2)]. The placement of the detectors was checked at the beginning, but not at the end of the measurement sessions; therefore, an accurate correction factor for the measurements around the skull is not possible. A similar issue may affect the data for the knees, but the effect is an order of magnitude smaller: the simulations showed a decrease in the counting efficiency of at most 7 % for a slide of 2 cm.

Table 1. Activities calculated for the mixed configuration, according to the calibration phantom used.

Organ	ICRP Female [Bq]	ICRP Man [Bq]
Skeleton[a]	152	288
Lung left[b]	60	73
Lung right[b]	59	77
Liver	0	0

[a]Based on knee measurements.
[b]The calibration phantom did not distinguish between lung and thoracic lymph nodes.

Table 2. Activities calculated for the skeleton-specific configuration, according to the calibration phantom used.

Organ measured	ICRP Female [Bq]	ICRP Man [Bq]
Knee	103	216
Knee	141	270
Average knees	122	243
Skull left	176	556
Skull right	184	449
Average skull	180	503

INTERPRETATION OF MEASUREMENTS

This inhalation case has been analysed in the past by different authors and has been used in an internal dosimetry inter-comparison exercise(5). The analysis did show a very long lung retention, which could only in part be accounted for by assuming that the inhaled material was very insoluble. A significantly slower particle transport clearance mechanism in the lungs had also to be assumed in order for the model predictions to agree with the measurements.

The data have been analysed here, by using the following models:

- for deposition, particle transport and absorption to blood in the respiratory tract, a revision of the Human Respiratory Tract Model (HRTM)(6). In the revised particle transport model, the material deposited in the alveolar compartment clears to the bronchial tree at a rate of $m_T = 0.002\ d^{-1}$ and to the interstitial compartment at a rate of $m_I = 0.001\ d^{-1}$. The interstitial compartment clears very slowly to the regional lymph nodes at a rate of $0.00003\ d^{-1}$;
- for transit through the alimentary tract the ICRP-30 model(7);
- for systemic biokinetics, the Leggett model for plutonium(8) and the ICRP model for americium(9).

The isotopic composition of the inhaled aerosol was estimated from measurements in January 1983 (4 months before the accident) on the fuel samples used in the solution that was overheated and spread out in the accident. The alpha activity composition is recorded as 10 % ^{241}Am, 9 % ^{238}Pu, 55 % ^{239}Pu and 26 % ^{240}Pu. The ^{241}Pu (beta) activity is 750 % of the total alpha activity. The uncertainty on these measurements is not known. The above isotopic composition is consistent with the activity ratio $(^{238}\text{Pu} + {}^{241}\text{Am})/(^{239}\text{Pu} + {}^{240}\text{Pu}) = 0.24 \pm 0.05$ calculated from the early faecal samples. There are no faecal measurements for ^{241}Pu, but a previous laboratory record gives the ^{241}Pu activity as 655 % of the total alpha activity whereas all the alpha activities are within a few per cent from the values given above. The reason of the discrepancy for ^{241}Pu is not known.

As in the previous analysis, an effective AMAD(10) (Activity Median Aerodynamic Diameter) of ~5 μm has been estimated from early lung and early faecal excretion data (including the activity that would have appeared in the faeces if it had not been not removed with a nasal swab and a bronchial slime before the first chest measurement was done(1)). This value has been used to calculate the fractions of material

deposited in each of the lung regions. The calculated activity deposited in the nasal region has been adjusted by subtracting the amount that was removed immediately after the intake by nose swab. This correction does not affect the estimate of the effective dose but only the fit to the very early faecal data.

Particles deposited in the lungs are cleared by two competing mechanisms, by particle transport (to the gut and to the lymph nodes) and by absorption to blood of the dissolving material. For the latter, f_r indicates the fraction dissolved rapidly at the rate s_r, whereas the complementary fraction $(1 - f_r)$ is dissolved slowly at the rate s_s. A fraction f_b of the dissolved material may not be absorbed directly into blood and could bind temporarily ($s_b > 0$) or permanently ($s_b = 0$) to lung tissues. As mentioned, the fraction $(1 - f_b)$ is available to be absorbed to blood at the rates s_r and s_s.

Absorption of material from the respiratory tract to blood was shown to be slow in previous analysis. The inhaled material was initially assumed to be 'type S' solubility[11], with absorption parameter values: $f_r = 0.001$, $s_r = 1\ d^{-1}$, $s_s = 0.001\ d^{-1}$, and a bound state was assumed with $f_b = 0.002$ and $s_b = 0\ d^{-1}$[6, 12]. Note that the bound state does not play a significant role in the long-term retention in the lungs because the material is relatively insoluble. The gut uptake fraction was kept fixed to its default value of $f_1 = 5\ 10^{-4}$ for type S material.

Measurement errors were assumed to be log-normally distributed. The geometric standard deviations, or scattering factors, for the different datasets were either estimated from the data, as described by Marsh *et al.*[13], or based on the default values given in the IDEAS guidelines[10]. The values for the scattering factors were 1.2, 1.6 and 2.4 for chest, urine and faecal measurements and 2 for liver and skeleton.

The agreement between measurements and model predictions was poor when using default parameter values, and the following changes to the models were introduced to improve the fit to the data:

- the particle transport in the alveolar–interstitial region was reduced;
- the absorption parameter values of the inhaled material were optimised, either assuming that they were the same for Am and Pu (i.e. shared values) or that they were different (i.e. independent);
- the isotopic activity composition was allowed to vary;
- the transfer rates from blood to urinary bladder were varied in order to improve the fit to the skeleton and liver measurements.

The changes were applied by finding optimal model parameter values using the maximum-likelihood method. To address first the issue of activity balance, only chest and excretion data were used. Liver and skeleton data were included only in the last stage of the optimisation. The agreement between model prediction and measurements improved significantly, in terms of chi-squared, for each of the above changes (Table 3).

Table 3. Lung absorption parameters, committed effective dose (CED) and organ doses (equivalent doses and per cent contribution to the effective dose) for each added changes in the optimisation.

	PT + AbsP	+ isotopic composition	+ Blood–UB
f_r (Pu)	0.0014	0.0017	0.004
f_r (Am)	0.05	0.04	0.08
s_r (d^{-1})	0.21	0.19	0.32
s_s ($10^{-5}\ d^{-1}$)	5	5	7
CED (Sv)	1.3	1.1	1.2
Lung [Sv (%)]	8.3 (77)	6.8 (74)	6.3 (67)
Liver	2.3 (7)	2 (7)	3 (10)
Bone surface	10 (8)	9 (8)	14 (12)
R.B.M.	0.5 (5)	0.5 (5)	0.7 (7)
χ^2_{TOT} (236 data)	261	232	212[a]
χ^2_{LUNG} (17 data)	38	16	12

[a]242 data, including skeleton (3) and liver (3) data.

The adoption of the revised HRTM model[6] improves the fit to lung and faecal excretion data, compared with the previous HRTM[11], but a further reduction of the particle transport rate from the alveolar region to the bronchiolar needs to be applied, from $m_T = 2 \times 10^{-3}\ d^{-1}$ to $m_T = 3 \times 10^{-4}\ d^{-1}$. The optimal value for the rate to the interstitial regions (m_I=$8.5 \times 10^{-4}\ d^{-1}$) differs only slightly from the default value ($m_I = 1 \times 10^{-3}\ d^{-1}$). The changes may also be expressed as an increase of the so-called sequestered fraction in the alveolar–interstitial region, $m_I/(m_I + m_T)$ from 0.33 to 0.74 and in the slowdown of the clearance to the gut. This value is relatively high but close to the upper limit of the 68 % probability range for the inter-subject variation: (0.2, 0.7)[14]. Assuming that americium is more soluble than plutonium in the lungs improves the overall prediction for urine excretion, although the very late americium excretion remains slightly overestimated. The rapid and slow absorption rates s_r and s_s for plutonium are not well determined by the data, and it would be possible to assume the same values of s_r and s_s (shared values) for both Am and Pu without affecting significantly the fit to the data. However, a much better fit is obtained when the values for the rapid fraction f_r are optimised independently. The optimal shared values are $s_r = 0.2\ d^{-1}$ and $s_s = 5 \times 10^{-5}\ d^{-1}$, and $f_r = 0.0014$ for Pu and $f_r = 0.05$ for Am. The result might be interpreted as an indication that

initially americium dissolves faster. Americium oxide is generally more soluble than plutonium oxide[15], but it is usually also considered that the rate at which a particle dissociates is determined by the particle matrix and therefore the dissolution parameter values for americium and plutonium should be similar if they belong to the same matrix. An interpretation of the above result could possibly be provided by a better knowledge of the physicochemical properties of the inhaled material.

The overall fit is not sufficiently good, and this is mainly due to the model prediction being 'pulled' in opposite directions by chest and urine data.

An estimate of the isotopic composition of the inhaled material is necessary to determine the initial amount of americium and plutonium (isotopes) deposited in the lungs. The values given above have been considered as fixed in previous analysis. Based on the available information, the authors assumed here a relative error of 10 % and used it for a constrained optimisation. This would be equivalent to introduce a prior distribution for the isotopic fractions within a Bayesian framework.

The result of the optimisation, 13 % ^{241}Am, 9 % ^{238}Pu, 53 % ^{239}Pu, 25 % ^{240}Pu and 660 % ^{241}Pu, shows that the complete set of data and the models used might be more consistent with a different isotopic composition. However, the ratio (^{238}Pu + ^{241}Am)/(^{239}Pu + ^{240}Pu) = 0.25 is still compatible with the estimate 0.24 ± 0.05 based on the early faecal measurements. The lower beta activity (^{241}Pu) also cannot be completely excluded because of the two different values given in the laboratory records.

The previous adjustments to the models improve significantly the overall agreement between model prediction and experimental data, except for liver and skeleton. The reasons for the discrepancy could be various, but to improve the fit to the liver and skeleton data, it is necessary to modify systemic parameter values. A sensitivity analysis shows that reducing the amount transferred from blood to bladder is the most effective in ensuring a good fit to the two systemic organ datasets and improving further the agreement with the urine data. The main effect is an increase of the dose to internal organs, because more activity is retained in the body instead of being excreted through urine, and an adjustment of the lung absorption parameters. Note that this effect is achieved even if liver and skeleton data are not included in the fitting because it is mainly driven by the urine data. The rates from blood to urinary bladder have been changed by keeping constant the removal half-time from blood. A constraint equivalent to a lognormal prior distribution with geometric standard deviation equal to log(1.7)[16] has been applied in the optimisation.

Table 3 shows how the optimal parameter values, doses and chi-squared did vary when the changes [particle transport (PT) plus absorption parameters (AbsP), isotopic composition, blood to urinary bladder] were applied sequentially.

LUNG ABSORPTION PARAMETERS

The maximum-likelihood procedure used for the parameters estimation indicates that the shared parameter s_r and f_r for Pu are less well defined by the data than the other parameters. The estimates of f_r, s_r and s_s are not significantly correlated between them ($|\rho| < 0.15$) but show higher correlation with the estimate of the blood-to-urinary bladder rate.

The uncertainty on the estimates of the lung absorption parameters has been further investigated by using Bayesian Markov chain Monte Carlo sampling[17]. Lognormal prior distributions have been assumed for the parameters, which were constraint in the optimisation. 'Non-informative' priors (normal distribution for the log-transformed variable with $\sigma = 2$ and centred on the best-fit result) have been used for all the other parameters. Most of the absorption parameters were well defined (Table 4) as the posterior distribution was relatively narrow (compared with the prior distribution) and approximately centred on the best-fit value. The exceptions are the fast-absorbed fraction f_r for plutonium, for which only an upper limit ($f_r < 0.015$) is clearly defined, and for the shared parameter s_r for which the lower limit is better defined than the upper limit ($s_r > 0.2$ d^{-1}). All set of measurements used in the analysis are given in the Annex (Tables A1–A5). Figures 1–4 show measurements and best-fit model predictions for a subset of the datasets. As shown in Figure 1, most of the ^{241}Am activity predicted in chest at later times is due to in-growth from ^{241}Pu.

CYTOGENETIC ANALYSIS

In addition to the biokinetic modelling, three different cytogenetic assays have been performed to analyse diverse biomarkers of exposure in blood lymphocytes.

Dicentric assay

Up to now, the conventional analysis of dicentric chromosomes (dicentric assay) is the most appropriate

Table 4. MCMC results for lung absorption parameters and CED.

	Mean value	95 % probability interval
f_r (Am)	0.08	0.04–0.12
f_r (Pu)	0.003	<0.015
s_r (d^{-1})	0.4	0.17–5
s_s (d^{-1})	8×10^{-5}	6×10^{-5}–1×10^{-4}
CED (Sv)	1.2	1.0–1.35

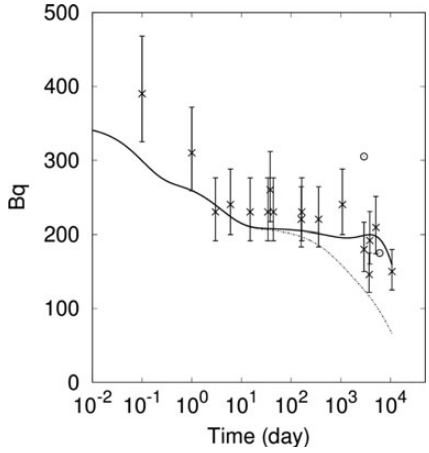

Figure 1. ^{241}Am in chest. The dash-dotted curve shows the predicted ^{241}Am activity without taking into account of in-growth from ^{241}Pu.

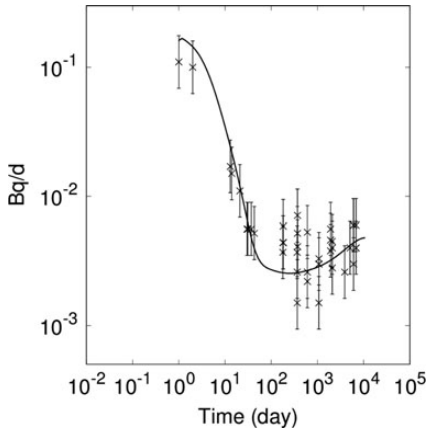

Figure 2. ^{241}Am + ^{238}Pu in 24-h urine excretion.

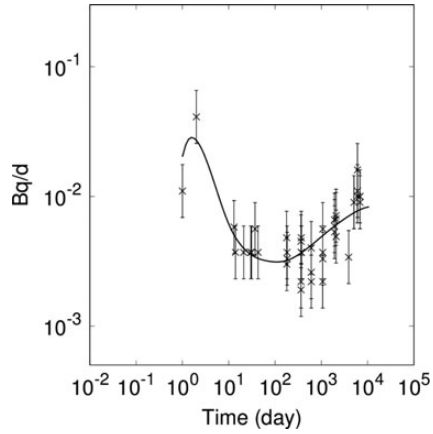

Figure 3. ^{239}Pu + ^{240}Pu in 24-h urine excretion.

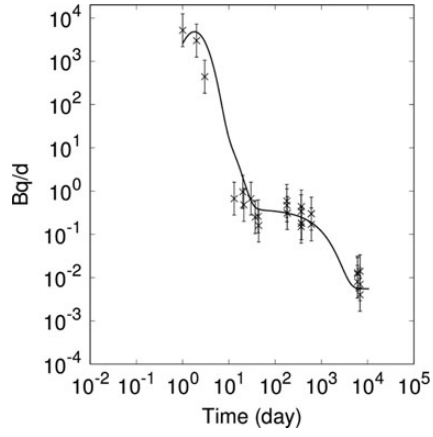

Figure 4. ^{239}Pu + ^{240}Pu in 24-h faecal excretion.

assay to estimate a dose in case of an acute irradiation[18, 19]. This assay was also used in a previous examination of the same person years ago[1]. In the present study, a total of 1000 cells from Giemsa stained slides were analysed. The observed frequency of 2 dicentric chromosomes per 1000 cells was not significantly different ($p > 0.05$) in comparison with the authors' control value of 1.15 dicentric chromosomes per 1000 cells. This result was to be expected because of the 30-y time period between the first accidental exposure and the current blood sampling. The biological half-life of lymphocytes with dicentric chromosomes is assumed to be 3 y. Due to a detriment of dicentric chromosomes during cell division, the yield of lymphocytes in the circulating blood bearing this biomarker will decrease in the course of time.

FISH assay (symmetrical translocations)

The yield of symmetrical translocations in 3017 cells scored was significantly increased (23.8 ± 5.0/1000 cells, FG (Genome equivalents) values) in comparison with an age-adjusted control group including 35 persons and 88 934 cells scored [7.5 ± 0.51/1000 cells, FG (Genome equivalent) values]. This aberration type has the advantage to pass cell division without major detriment and thus is more persistent. In consequence, symmetrical aberrations are the indicator of choice for past and chronic radiation conditions[20]. In the current case, the significant increase of symmetrical translocations indicates an irradiation incident. Because of the lack of an appropriate dose–effect curve for this radiation quality (alpha particles) and the extreme long time period since the exposure, a dose reconstruction was considered to be not feasible.

Micronucleus assay

For micronuclei, the increase observed in comparison with the unexposed control group was ambiguous. In fact, there was a significant increase in the mean value of micronuclei compared with the control value; however, there still was an overlap with the upper dose interval of the non-irradiated control. The reason is the relatively high and variable spontaneous frequency of micronuclei in control cells, which tends to increase with age and also shows gender dependency[21]. Additionally problematic is the lack of specificity of micronuclei, as they can also be caused by chemical clastogenic agents. Therefore, the increase found here cannot clearly be assigned to the radiation accident; however, a relationship cannot be excluded.

In summary, the significant increase of symmetrical aberrations, while no enhancement of dicentric chromosomes is observed, provides evidence for a past radiation exposure of the blood forming tissue and/or ongoing chronic low dose exposure.

CONCLUSION AND OUTLOOK

The Pu/Am inhalation case of 1983 has been studied by colleagues in several institutions and described in numerous papers including the publication of 2007[1], the actual publication and many papers cited in both publications. The aim of the full publication of all data of this case is to make this information available for internal dosimetry model evaluation and training in internal dosimetry. It will depend on the availability and willingness of the person involved whether the series of measurements can be continued and the results presented in a future update.

ACKNOWLEDGEMENTS

The authors thank the person who has suffered the Pu/Am inhalation in 1983 for his continued willingness to cooperate in all the studies performed. They also thank the medical service of the Swiss Social Insurance Fund (Suva) for the recent general medical check-up, which fortunately attested good health of the person.

REFERENCES

1. Wernli, C. and Eikenberg, J. *Twenty-year-follow-up of a Pu/Am inhalation case*. Radiat. Prot. Dosim. **125**(1–4), 506–512 (2007).
2. Marzocchi, O. *Design and setup of a new HPGe detector based body counter capable of detecting also low energy photon emitters*. University of Bologna, Thesis. Chapters 4.3; 5; 6.2, (2011).
3. Stephan, G., Oestreicher, U. and Romm, H. *Biological dosimetry*. In: Chromosomal Alterations—Methods, Results and Importance in Human Health. Obe, G. and Vijayalaxmi, Eds. Springer, pp. 341–349 (2007).
4. Pelowitz, D. B. (ed.), *MCNPX User's Manual Version 2.7.0*. Los Alamos National Laboratory, (2011). LA-CP-11-00438.
5. IAEA. IAEA-TECDOC-1568. *Intercomparison Exercise on Internal Dose Assessment*. IAEA, (2007).
6. ICRP. *Occupational intakes of radionuclides, Part 1. Annals of the International Commission on Radiological Protection*, Accepted for publication, (2014a).
7. ICRP. *Limits for intakes of radionuclides by workers ICRP publication 30 (Part 1)*. Ann. ICRP 2 (3–4), (1979).
8. Leggett, R. W. *et al. Mayak worker study: an improved biokinetic model for reconstructing doses from internally deposited plutonium*. Radiat. Res. **164**(2), 111–122 (2005).
9. ICRP. *Age-dependent doses to members of the public from intake of radionuclides: Part 2. Ingestion dose coefficients. A report of a Task Group of Committee 2 of the International Commission on Radiological Protection*. Annals of the ICRP, 23(3–4), pp. 1–167 (1993).
10. Castellani, C., Marsh, J. and Hurtgen, C. *IDEAS Guidelines (Version 2) for the estimation of committed doses from incorporation monitoring data*. (2013). Available on http://www.eurados.org/~/media/Files/Eurados/documents/EURADOS%20Report%202013-01%20online%20version.pdf [Accessed June 27, 2014].
11. ICRP. *Human respiratory tract model for radiological protection. A report of a Task Group of the International Commission on Radiological Protection*. Annals of the ICRP, 24(1–3), pp. 1–482 (1994).
12. ICRP. *Occupational intakes of radionuclides, Part 4. Annals of the International Commission on Radiological Protection*, in progress (2014).
13. Marsh, J. W. *et al. Evaluation of scattering factor values for internal dose assessment following the IDEAS guidelines: preliminary results*. Radiat. Prot. Dosim. **127**(1–4), 339–342 (2007).
14. Gregoratto, D., Bailey, M. R. and Marsh, J. W. *Modelling particle retention in the alveolar-interstitial region of the human lungs*. J. Radiol. Prot. **30**(3), 491–512 (2010).
15. ICRP. *Dose coefficients for intakes of radionuclides by workers*. ICRP Publication 68. Ann. ICRP 24 (4) (1994b).
16. Puncher, M. and Harrison, J. D. *Uncertainty analysis of doses from ingestion of plutonium and americium*. Radiat. Prot. Dosim. **148**, 284–296 (2012).
17. Gelman, A. and Rubin, D. B. *Markov chain Monte Carlo methods in biostatistics*. Stat. Methods Med. Res. **5**(4) 339–355 (1996).
18. International Atomic Energy Agency. *Cytogenetic dosimetry: applications in preparedness for and response to radiation emergencies*. EPR-Biodosimetry 2011. IAEA (2011).
19. Romm, H., Oestreicher, U. and Kulka, U. *Cytogenetic damage analysed by the dicentric assay*. In: Biodosimetric tools for a fast triage of people accidentally exposed to ionising radiation. Ann. Ist Super Sanità. **45**, 251–259 (2009).
20. Ainsbury, E. A., Bakhanova, E., Barquinero, J. F., Brai, M., Chumak, V., Correcher, V., Darroudi, F., Fattibene, P., Gruel, G., Guclu, I. *et al. Retrospective dosimetry techniques for external radiation exposures*. Radiat. Prot. Dosim. **147**, 573–592 (2011).
21. Fenech, M. *The cytokinesis-block micronucleus technique: a detailed description of the method and its application to genotoxicity studies in human populations*. Mutat. Res. **285**, 35–44 (1993).

ANNEX

Table A1. Chest[a], faeces and urine measurements: ^{241}Am.

Chest		Faeces		Urine	
t (d)	Bq	t (d)	Bq d^{-1}	t (d)	Bq d^{-1}
0.1	390	1074	0.0180	2092	0.0023
1	310	1075	0.0300	2095	0.0036
3	230	1076	0.0170	2525	<0.0015
6	240	1077	0.0070	2526	0.0051
15	230	1921	0.0130	2527	0.0034
34	230	1922	0.0460	2921	0.0027
38	260	1923	0.0150	2922	0.0019
44	230	2525	0.0170	2923	<0.0015
160	220	2526	0.0050	6043	0.0050
164	230	2527	0.0130	6044	0.0020
357	220	2921	<0.0015	6045	0.0050
1077	240	2922	0.0060	6859	0.0050
2925	180	2923	<0.0015	6860	0.0030
2926	305[b,c]	6043	0.0040	6861	0.0030
3724	146[c]	6044	0.0040	6870	0.0030
3828	192[c]	6045	0.0020	6903	0.0021
5078	209[c]	6859	0.0010	10708	0.0049
6037	175[b,c]	6860	0.0020	10709	0.0019
10713	150[d]	6861	0.0020	10710	0.0016
		10708	0.0023		
		10709	0.0004		
		10710	0.0021		

[a]Chest measurements may include counts from thoracic lymph nodes, ribs and liver.
[b]Data that have been excluded from the fitting.
[c]Lung and lymph node activities were measured separately and added together.
[d]See text for description of measurement.

Table A2. Liver and skeleton measurements: ^{241}Am.

Liver		Skeleton	
t (d)	Bq	t (d)	Bq
2926	27	2926	57
3724	57[a]	3724	69
3828	24	3828	65
5078	17	5078	95
		6037	95
10713	0	10713	243[a]

[a]Data that have been excluded from the fitting.

Table A3. Faeces and urine measurements: ^{238}Pu + ^{241}Am.

Faeces		Urine	
t (d)	Bq d^{-1}	t (d)	Bq d^{-1}
1	1500.000	1	0.1100
2	740.000	2	0.1000
3	74.000	13	0.0170
13	0.160	14	0.0150
20	0.190	21	0.0110
21	0.110	30	0.0056
30	0.120	31	0.0056
37	0.078	37	0.0056
43	0.074	43	0.0052
44	0.044	179	0.0037
179	0.120	180	0.0044
180	0.100	182	0.0059
182	0.093	183	0.0044
183	0.063	364	0.0037
365	0.081	365	0.0026
366	0.026	366	0.0015
369	0.110	369	0.0052
370	0.037	370	0.0071
371	0.041	371	0.0041
605	0.085	605	0.0026
606	0.080	606	0.0053
607	0.059	607	0.0022
6043	0.005	1074	0.0015
6044	0.005	1075	0.0033
6045	0.002	1076	0.0030
6859	0.001	1077	0.0030
6860	0.003	1921	0.0056
6861	0.003	1922	0.0046
		1923	0.0038
		2089	0.0045
		2090	0.0040
		2091	0.0028
		3902	0.0026
		5076	0.0040
		6043	0.0060
		6044	0.0030
		6045	0.0060
		6859	0.0060
		6860	0.0040
		6870	0.0040

Table A4. Faeces and urine measurements: $^{239+240}$Pu.

Faeces		Urine	
t (d)	Bq d^{-1}	t (d)	Bq d^{-1}
1	5200.000	1	0.0110
2	3000.000	2	0.0410
3	440.000	13	0.0058
13	0.670	14	0.0037
20	0.960	21	0.0037
21	0.480	30	0.0037
30	0.670	31	0.0037
37	0.250	37	0.0056
43	0.260	43	0.0037
44	0.160	179	0.0048
179	0.590	180	0.0030
180	0.470	182	0.0037
182	0.310	183	0.0033
183	0.310	364	0.0045
365	0.340	365	0.0022
366	0.150	366	0.0019
369	0.440	369	0.0037
370	0.180	370	0.0048
371	0.180	371	0.0037
605	0.300	605	0.0026
606	0.300	606	0.0040
607	0.170	607	0.0022
6043	0.012	1074	0.0022
6044	0.013	1075	0.0037
6045	0.008	1076	0.0033
6859	0.004	1077	0.0056
6860	0.014	1921	0.0059
6861	0.007	1922	0.0053
		1923	0.0066
		2089	0.0071
		2090	0.0049
		2091	0.0067
		3902	0.0034
		5076	0.0090
		6043	0.0110
		6044	0.0100
		6045	0.0160
		6859	0.0100
		6860	0.0100
		6870	0.0090

Table A5. Faeces and urine measurements: $^{238+239+240}$Pu.

Faeces		Urine	
t (d)	Bq d^{-1}	t (d)	Bq d^{-1}
1074	0.0700	2525	0.0042
1075	0.1200	2526	0.0064
1076	0.0650	2527	0.0070
1077	0.0250	2921	0.0047
1921	0.0900	2922	0.0044
1922	0.1900	2923	<0.0015[a]
1923	0.1000	3723	0.0100
2525	0.0470	3725	0.0090
2526	0.0170	6043	0.0130
2527	0.0380	6044	0.0100
2921	0.0050	6045	0.0170
2922	0.0130	6859	0.0100
2923	0.0030	6860	0.0100
3723	0.0150	6861	0.0090
3725	0.0110	6870	0.0100
6043	0.0130	6903	0.0090
6044	0.0140	10708	0.0090
6045	0.0090	10709	0.0054
6859	0.0040	10710	0.0040
6860	0.0140		
6861	0.0080		
10708	0.0060		
10709	0.0017		
10710	0.0063		

[a]Data that have been excluded from the fitting.